

DETERMINATION OF NEWTON'S GRAVITATIONAL
CONSTANT, G, WITH IMPROVED PRECISION

Status Report
covering the period
1 April 1965 - 30 September 1965
under NASA Grant NGR-47-005-022

NASA CR70779

Principal Investigators
J. W. Beams
Department of Physics

A. R. Kuhlthau
R. A. Lowry
H. M. Parker

Department of Aerospace Engineering
and Engineering Physics

GPO PRICE \$ _____
CFSTI PRICE(S) \$ _____
Hard copy (HC) 2.00
Microfiche (MF) .50

653 July 65

Research Laboratories for the Engineering Sciences
University of Virginia
Charlottesville

FACILITY FORM 802

N66-19657
(ACCESSION NUMBER) (THRU)
31
(PAGES) (CODE)
CR 70779
(NASA CR OR TMX OR AD NUMBER) (CATEGORY)
23

J

Report No. EP-4028-102-65U
December 1965

DETERMINATION OF NEWTON'S GRAVITATIONAL CONSTANT,
G, WITH IMPROVED PRECISION

Status Report
covering the period
1 April 1965 - 30 September 1965
under NASA Grant NGR-47-005-022

Principal Investigators

J. W. Beams

Department of Physics

A. R. Kuhlthau

R. A. Lowry

H. M. Parker

Department of Aerospace Engineering
and Engineering Physics

RESEARCH LABORATORIES FOR THE ENGINEERING SCIENCES
SCHOOL OF ENGINEERING AND APPLIED SCIENCE
UNIVERSITY OF VIRGINIA
CHARLOTTESVILLE, VIRGINIA

Report No. EP-4028-102-65U
December 1965

Copy No. 5

TABLE OF CONTENTS

		Page
SECTION I	INTRODUCTION	1
	Model A-1 and A-2 Magnetic Support	3
	Model B - Torsion Fiber	3
SECTION II	CURRENT STATUS OF THE PROGRAM	5
	A. Task I - Theoretical Analysis	5
	1. Geometry and Density Variations	5
	2. Equation of Motion	5
	3. Design of the Mass Systems	6
	B. Task II - Apparatus Design and Procurement of Components	11
	1. Large Mass System	12
	2. Small Mass System	12
	3. Rotary Table	13
	4. Servo Drive System	13
	5. Measurement of Period of Rotation of Rotary Table	16
	6. Suspension - Model B	17
	7. Suspension - Model A	17
	8. Dust-Free Facility	17
	C. Task III - Assembly of Apparatus and Development of Techniques	17
	1. Prototype Apparatus	17
	2. Metrology	19
SECTION III	STAFF	21
SECTION IV	EXPENDITURES	23
	REFERENCES	25

LIST OF ILLUSTRATIONS

		Page
FIGURE 1	SCHEMATIC OF APPARATUS	2
FIGURE 2	GEOMETRY OF INTERACTING SYSTEMS.	7
FIGURE 3	F (x β) vs. β where	
	$F(x\beta) = \frac{\sin\beta}{x} [(1 + x^2 - 2x \cos\beta)^{-3/2} - (1 + x^2 - 2x \cos\beta)^{-3/2}]$. . . 9
FIGURE 4	SERVO DRIVE FOR PRECISION RATE TABLE	14
FIGURE 5	PROTOTYPE ASSEMBLY.	18

SECTION I INTRODUCTION

This is the second semi-annual status report under this grant, the object of which is to apply new techniques to the laboratory determination of the Newtonian Gravitation Constant, G , with the expectation of improvement of the accuracy by about two orders of magnitude. The improvement is attributed to both a new approach to the measurement, which should eliminate or bring under better control most of the difficulties encountered in earlier methods, and to improvements in materials, metrology, fabrication procedures, etc. which should circumvent many problems and limitations previously encountered.

With reference to the schematic diagram of Figure 1, two small masses, m , are connected by a rigid horizontal rod. These are then placed in proximity to another pair of masses, M , and the gravitational interaction between the two sets of masses results in a pure torque acting on the m -system. A measure of this torque plus a knowledge of the separation distance, d , enables G to be determined. Previous experimenters either measured the torque directly by observing the static deflection of a torsion fiber suspension or introduced variations on this method such as inducing resonant torsional oscillations in the m -system by suitably driving the large M system.

In the present proposed method the gravitational torque is maintained constant by detecting changes in the relative angular position β of the two mass systems and correcting the relative position by a servo mechanism to maintain β constant to the necessary accuracy. Thus the nearly constant torque being applied to the m -system results in a nearly constant angular acceleration of this system which can be permitted to act for an extended period of time. The ultimate measurement, then, is one of determining the angular speed of the m -system at the end of this extended period of time, i. e., of measuring large displacements and long times, both of which can be done accurately.

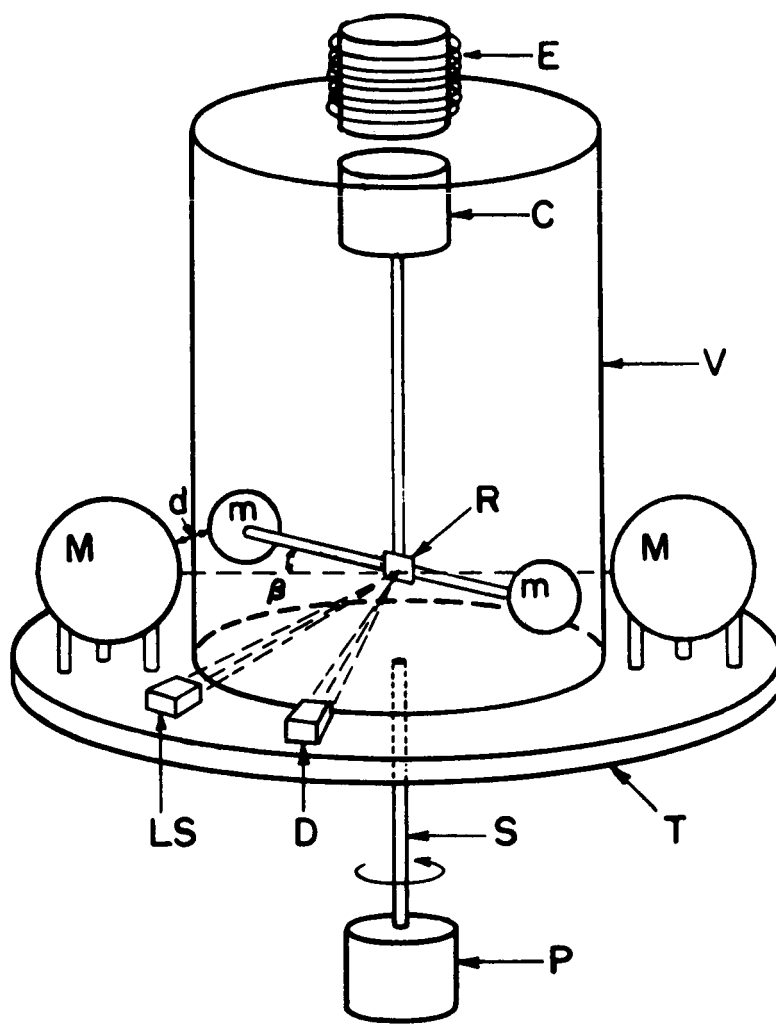


FIGURE 1

SCHEMATIC OF APPARATUS

In designing the experiment, three methods for suspending the m-system have been considered. Two of these involve the use of magnetic suspensions and for future reference these will be designated Models A-1 and A-2. The other involves the use of a more conventional torsion fiber and this will be designated as Model B. Each system has many advantages and disadvantages in comparison with the others, and in fact it is at this stage impossible to make the final selection. They are all being studied more carefully as part of the initial phases of the program, and working models of each design are being constructed and evaluated.

For the orientation of the reader, the principal differences are:

Model A-1 and A-2 - Magnetic Support

Again referring to Figure 1, the center of the rod connecting the small masses, m, is attached to a rigid vertical rod containing at its upper end, a small cylinder of magnetic material, C. This is freely suspended by the electromagnet E [1]. The major advantage of the electromagnetic suspension models is that the precision to which the angle β must be held constant in order to get the desired precision in the determination of G is only 10^{-3} radians, an easy prospect. The major disadvantage is the rather elaborate magnetic shielding required.

In Model A-1 the coil of the electromagnet E, is attached to the rotating table.

In Model A-2 the coil of the electromagnet is free of the rotating table and is fixed in the laboratory frame of reference.

The advantages and disadvantages between these two versions are more subtle. They are discussed in more detail in reference [2], and for the present purposes it need only be said that they do exist, are significant, and can only be evaluated by further experimentation.

Model B - Torsion Fiber

Model B replaces the electromagnetic suspension with a delicate torsion fiber mounted from the rotating table. As the m-system begins to rotate as a

result of its interaction with the M system, the fiber support is rotated, due to the table rotation, and the balance always operates at essentially constant deflection (which will be as close as possible to the null point). The major disadvantage here is that this deflection angle and β , must be held constant to 10^{-6} radians in order to get accuracy in the G measurement comparable to what can be obtained by knowing β to 10^{-3} radians in the case of the magnetic support. The big advantage, of course, is the elimination of the magnetic field, and hence a minimization of magnetic effects.

At the present time the program is divided into three principle tasks, the status of each of which is summarized in the following sections. These tasks are:

1. Theoretical Analysis
2. Apparatus Design - Details and Procurement of Components
3. Assembly of Apparatus and Development of Techniques

SECTION II
CURRENT STATUS OF THE PROGRAM

A. Task 1 - Theoretical Analysis

The theoretical calculations can be grouped under three major categories.

1. Geometry and Density Variations

The first is the study of various sources of errors with the objective of reducing them to an analytical form suitable for experimental verification. If this can be successfully done, then corrections can usually be made in cases where the error cannot be adequately minimized through proper design. Most of these errors can be considered essentially as errors in geometry of the system, or as errors caused by the existence of density gradients in certain of the components of the apparatus. The results of approximate calculations of several such effects were reported in the previous progress report [3] and there is nothing further of significance to report at this time.

2. Equation of Motion

The differential equation describing the rotational motion of the m-system can be written as

$$(A) \quad \ddot{\theta} = a + \sum_i A_i \sin (2\theta + \phi_i).$$

where: a - represents the constant angular acceleration due to the m-M interaction and the interactions of the m-system with other masses fixed on the rotating table.

$A_i \sin (2\theta + \phi_i)$ - represents a typical term due to the interaction of the m-system with the masses fixed in the laboratory. There will be one such term for each mass which has a measurable influence on the motion.

The technique for solving this equation was developed on the basis of retaining only one term in the summation. The first integration is trivial and the second was shown to be straight forward if the cosine term resulting from the first integration is expanded in a series. It seemed reasonable that the result could be generalized to include i sinusoidal perturbation terms and it was proposed that the result could be written in the form

$$(B) t_n = \frac{\dot{\theta}_0}{a} \left[\sqrt{1 + \frac{4\pi na}{\dot{\theta}_0^2}} - 1 \right] + K_1 n + K_2 n^2 + \dots K_i n^i + \dots$$

when,

t_n is the time required to make n revolutions,

$\dot{\theta}_0$ is initial angular velocity,

K_i are functions of a, A_i, ϕ_i, θ_0 ,

It has now been verified that this approach is indeed valid and indications are that the series converges reasonably rapidly.

3. Design of the Mass Systems

A major effort during the period covered by this report has been a study of the optimum geometry and relative sizes of the interacting mass systems. To illustrate the nature of the problem, consider the idealized model as shown in Figure 2. In the actual apparatus there will be no direct line connection between the center of the large mass. There will be one between the small masses, but for the moment this connection is assumed to be massless. One now calculates the torque on each small mass due to the gravitational attraction of both large masses. All masses are assumed concentrated at their respective centers which is valid for spherical masses. If this torque is introduced into Newton's 2nd Law, the angular acceleration of the small mass system becomes (about the center of the system),

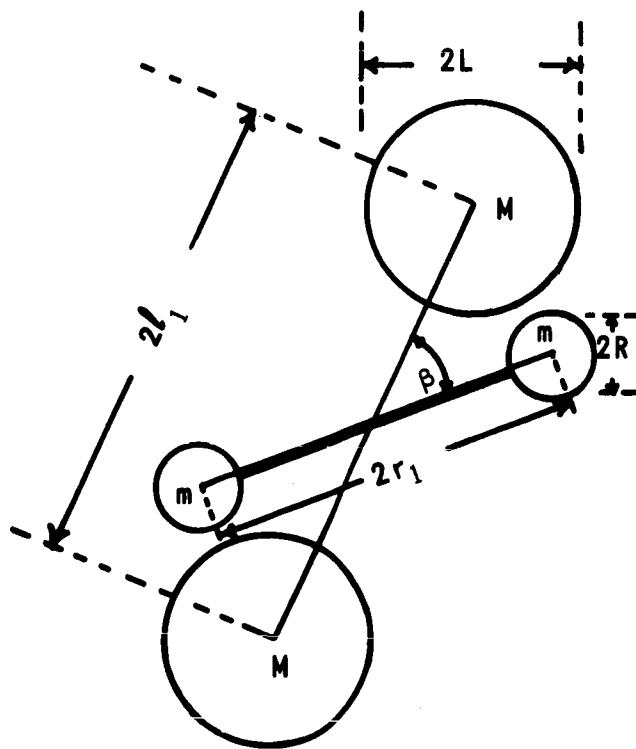


FIGURE 2
 GEOMETRY OF INTERACTING SYSTEMS

$$(B) \quad \frac{\dot{\omega}}{4/3 \pi \rho G} = \frac{\left(\frac{L}{\ell_1}\right)^3 F(x \beta)}{\left[1 + .4 \left(\frac{R}{r_1}\right)^2\right]}$$

where

$$x = \frac{r_1}{\ell_1} ,$$

ρ is the density of the large masses (assumed uniform),

G is the universal gravitation constant,

and the other terms are as defined in Figure 2.

Furthermore:

$$F(x\beta) = \frac{\sin \beta}{x} \left[(1 + x^2 - 2 x \cos \beta)^{-3/2} - (1 + x^2 + 2 x \cos \beta)^{-3/2} \right]$$

A plot of $F(x \beta)$ as a function of β for various values of x is shown in Figure 3. An interesting feature of this plot is the fact that the curves peak and $F(x \beta)$ and hence $\dot{\omega}$ is relatively insensitive to β in the vicinity of this maximum. For example at $x = 0.3$ an error of 0.1 degree in β will only cause an error of 1 part in 10^5 in $\dot{\omega}$ (and hence G).

It would also appear from the plot that there might be a compromise required between taking advantage of this flatness feature and obtaining the maximum $\dot{\omega}$. Fortunately this is not true. The term $\left(\frac{L}{\ell_1}\right)^3$ in the expression for $\dot{\omega}$ implicitly involves x , and in fact increases rapidly with decreasing x and thus far overshadows the reverse effect evident in $F(x \beta)$. We are of course interested in obtaining the maximum acceleration consistent with optimizing other considerations such as requirements on precision of measurement, ability to fabricate the apparatus, etc. Physically it is obvious that this will occur when the large masses

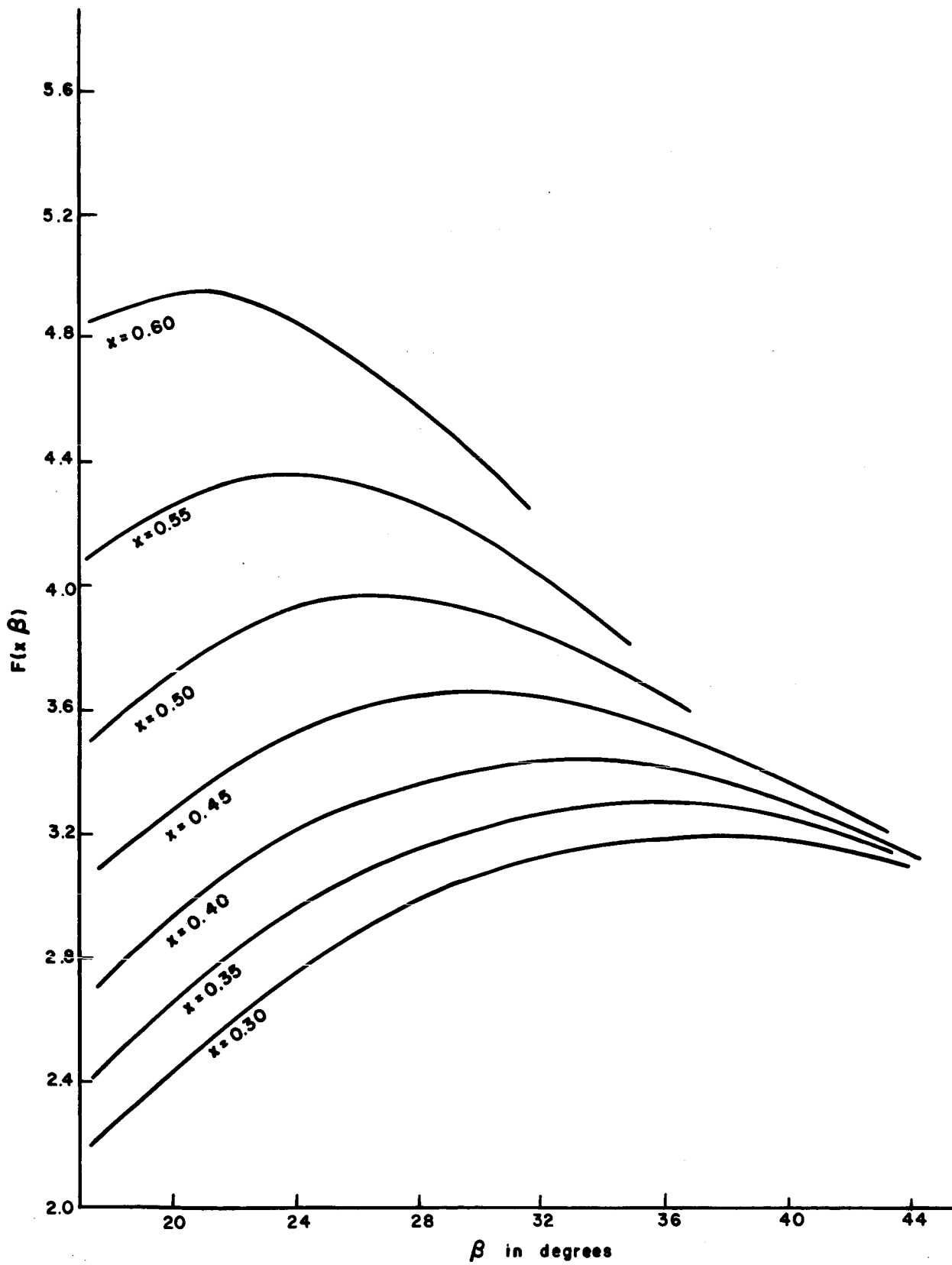


FIGURE 3

WHERE $F(x, \beta) = \frac{\sin \beta}{x} \left[(1+x^2 - 2x \cos \beta)^{-3/2} - (1+x^2 + 2x \cos \beta)^{-3/2} \right]$

are made as large as possible and their centers brought as close as possible to the adjacent small mass. However, all masses involved must be finite and practical considerations such as those mentioned above may well restrict the minimum dimensions of the small mass system. Thus the optimization must take account of geometrical limitations.

The performance of several models of particular interest was calculated in detail and the results are summarized in Table 1. In addition to the model illustrated in Figure 2, others were considered in which the large spherical masses were replaced with "long" cylinders (cylinder axis normal to the plane of the paper), or in which the small mass dumbbell is replaced by a rod. In both of these latter cases $F(x, \beta)$ is different from that in Figure 3, but the feature of the flat peak is preserved. Tungsten is assumed to be the material for the large mass system in calculating $\dot{\omega}$.

TABLE 1

Model No.	Type of Small Mass System	R in.	r_1 in.	x in.	Type of Large Mass	L in.	$\dot{\omega}$ rad/sec ²
1	dumbbell	0.1	0.225	2.25	spheres	2	0.93×10^{-5}
2	dumbbell	0.1	0.121	1.21	spheres	1	0.66×10^{-5}
3	dumbbell	0.1	0.252	2.52	spheres	2	0.68×10^{-5}
4	dumbbell	0.1	0.141	1.41	spheres	1	0.43×10^{-5}
5	dumbbell	0.1	0.262	2.62	spheres	2	0.61×10^{-5}
6	dumbbell	0.127	0.788	2.87	spheres	2	0.63×10^{-5}
7	dumbbell	0.127	0.788	3.16	spheres	2	0.38×10^{-5}
8	dumbbell	0.1	0.225	2.25	cylinders	2	1.04×10^{-5}
9	dumbbell	0.127	0.788	2.87	cylinders	2	0.91×10^{-5}
10	rod	---	0.225	2.25	spheres	2	0.93×10^{-5}

Several interesting conclusions can be drawn from Table 1.

- a) Models 5, 7, and 9 are the only three which have sufficient clearance between the two mass systems to allow the small mass system to be located inside the vacuum with the large mass system outside. By comparing 5 with 1, a considerable sacrifice in $\dot{\omega}$ must be paid for this feature.
- b) The small mass system used in Models 1-5 is quite small and causes some concern regarding the precision of measurement of the geometry of this system required by the small size. Models 6 and 7 represent a more reasonable size. Models 6 and 1 are directly comparable as are 7 and 5. Thus a price must also be paid in $\dot{\omega}$ if a larger size is desired.
- c) There is some concern that the cost of fabricating a 4" diameter large mass to high precision may become prohibitive. Thus some estimates were made for a large mass system of half of this diameter which should be considerably less expensive. The reduction in $\dot{\omega}$ (compare 2 with 1 or 4 with 3) is not as large as might have been expected.
- d) The use of cylinders in the large mass system will not produce much improvement in $\dot{\omega}$ for compact systems (compare 8 with 1) but is quite effective for the larger systems (compare 9 with 7).
- e) The replacement of the dumbbell with a solid rod in the small mass system leaves $\dot{\omega}$ essentially unchanged (compare 10 with 1).
- f) The absolute value of $\dot{\omega}$ for all models considered compared favorably with 0.2×10^{-5} rad/sec² which was the achievable value estimated in the original preliminary calculations leading to the proposal.

B. Task II - Apparatus Design and Procurement of Components

Discussions were held with various members of the Metrology Division of the National Bureau of Standards and with personnel at the Y-12 Plant of the U.S. Atomic Energy Commission operated by Union Carbide Corporation,

Nuclear Division, Oak Ridge, Tennessee concerning the detailed design of the various components of the large and small mass systems.

Included were such topics as

- size
- material
- fabrication techniques
- measurement of properties
- measurement of sizes
- alignment of components
- environmental control.

As a result of these discussions and our own calculations made to date it was possible to make several decisions as reported below concerning components. However, all of the problems are by no means solved and many of the details, particularly with regard to the last four items listed above, remain to be resolved.

1. Large Mass System

Although the calculations of the last section would tend to indicate that under certain circumstances there might be some advantage to using cylindrical masses, it is judged advisable not to do so unless other design considerations come to light which force one in this direction. This is due to the fact that there are some rather difficult fabrication and metrology problems involved with the cylinders. Consequently the decision has been made to use spheres, at least in the first model. A purchase order has been placed with the Y-12 Plant of the USAEC, Union Carbide Corporation, Nuclear Division for this work.

The matter of determining density gradients in the material is still under study.

2. Small Mass System

No definite action has yet been taken on the design of the small mass system. As a result of extensive discussions concerning the

fabrication, measurement and desirable properties of this system, the ideal of using a rod rather than the originally proposed dumbbell is receiving serious consideration. Since the density of the small mass system does not enter into the results of the measurement considerable latitude in the choice of material is available. Quartz appears as a current favorite as a result of detailed studies of possible precision fabrication procedures.

3. Rotary Table

A rotary table has been obtained from the Micrometrical Division of the Bendix Corporation. It has been installed and checked out using indicators good to a few microinches, and appears to meet the specifications. However, one disturbing factor was encountered in that the spindle bearing was much stiffer than had been imagined. The torque due to bearing friction with the table rotating in the range of the low speeds to be used in the experiment was about 20 oz-ins. This immediately gave rise to a problem with regard to the servo drive motor as discussed in the next section.

4. Servo Drive System

An A. C. torque motor was received from the Inland Motor Corporation near the end of July. Tests soon indicated that, due to the unexpectedly large bearing friction in the rotary table spindle, it would be inadequate for the job. As an immediate stop-gap solution, a larger model of this motor was ordered. However, the problem is by no means satisfactorily solved, since such things as motor heating, frequency response, etc. must still receive study.

The servo drive system is shown schematically in Figure 4.

The input to the servo amplifier is derived from the optical angle sensor (or optical lever) mounted on the rate table. Two photosensitive semiconductor diodes in the optical lever respond to unequal light intensities, thereby producing a voltage proportional to the angular variations from a preselected reference position between the two mass systems.

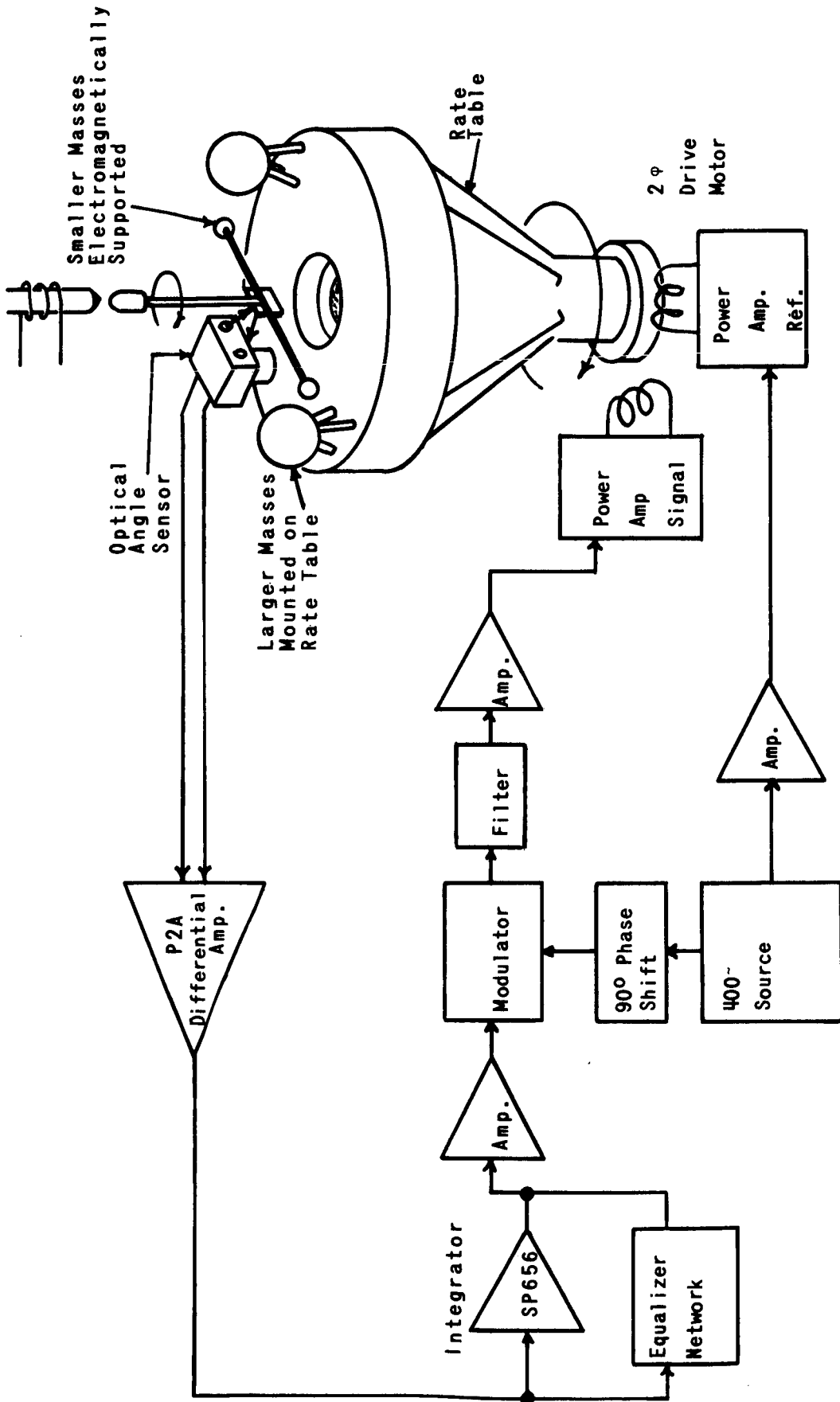


FIGURE 4
SERVO DRIVE FOR PRECISION RATE TABLE

4028'2

The error voltage is then fed to a differential operational amplifier (Philbrick P2A) which was specifically selected for its low noise, high gain with stability, and high common mode rejection ratio. The high common mode rejection ratio is needed to reduce fluctuations caused by variations of either the light source intensity or the voltage source supplying the photodiodes.

The single output from the differential amplifier is fed to the equalizer network and to an integrator circuit. A simple series equalizer network is shown in the diagram; at this stage of development the nature of the noise or disturbing inputs is not known to a degree to justify further sophistication.

It is expected that a relatively simple lead-lag network will suffice for stabilization. When more of the disturbances are known, the system will be optimized for maximum tracking accuracy, perhaps to the extent of adding separate channels or internal minor loop equalizers.

The need for the integrator circuit may be visualized by considering that the friction in the bearing of the rate table increases slightly, introducing a braking torque to the rate table which tends to slow it and hence cause it to lag behind the rotating reference. A small position error signal is produced and amplified by the differential amplifier and passed through the equalizer and eventually through the power amplifier to the motor, increasing the torque and preventing the angular error from increasing. As the amplification of this position information cannot be extremely large, a finite error would result were it not for the presence of the integrator. If the error signal exists for more than a few tenths of a second, a voltage proportional to the time integral is produced at the output of the integrator circuit and thus passes to the drive motor, reducing the error to insignificance.

The signals from the integrator and the equalizer network are fed next to another operational amplifier where they are mixed in the proper proportions and amplified to a suitable level for operating the modulator, as shown in Figure 4.

The operation of the series shunt solid state modulator may be understood by comparing it with a proportional "and" gate. An output signal from the modulator results only if both 400 cycle carrier frequency and the previously described error signal are present. The output is a 400 cycle carrier signal whose amplitude is proportional to the amplitude of the input error signal. The phase of the carrier is determined by the polarity of the error signal which is previously determined by the direction of the angular error.

The 400 cycle carrier frequency is produced by a 400 cycle oscillator with two outputs. One 400 cycle signal, which may be considered the reference output, is fed through a suitable power amplifier to one of the windings of the drive motor. The other signal, after its phase is shifted 90° , is amplified sufficiently to modulate the error signal as described above.

The 90° phase shift is necessary to produce a torque in the two phase AC motor where the torque is proportional to the sign of the angle between the two signals, reaching its maximum at 90° .

The amplitude of the reference signal on the motor may be set to any desired level. It will be set to a level consistent with the torque requirements necessary to overcome the friction of the bearing but as low as possible to prevent unnecessary heating of the motor which is connected directly to the shaft of the rate table.

The servomechanism is to rotate the rate table with such precision that a fixed position between the rate table and a rotating reference is maintained to within 10^{-5} radians.

5. Measurement of Period of Rotation of Rotary Table

The procedure for this measurement was described in some detail in the previous report. All components are now in hand and

the system will be evaluated as soon as the servo drive is installed on the rotary table and this complete unit is operative.

6. Suspension - Model B

This is the torsion fiber suspension. It has been constructed and installed on the rotary table. (See section C-1). Evaluation of the suspension and optical readout device is underway using non-precision components for the small and large mass systems. A detailed description of a similar Torsion suspension and optical lever arrangement can be found in references [4] and [5] .

7. Suspension - Model A

This is the model using the free electromagnetic suspension. The design of this apparatus including the servo control circuits is in advanced stages and construction has started on some of the components.

8. Dust-Free Facility

A clean room, manufactured by Agnew-Higgins Incorporated, was installed in early August and appears to operate very effectively. However, the problem of temperature control has not yet been resolved. As calculations continue and operational procedures are developed, it is obvious that reasonably good temperature control will ultimately be required to achieve the desired accuracy in the experimental measurements. Since this may become a rather crucial problem, and a relatively expensive one, it is difficult to develop an optimum design until all related factors, such as the heat generation in the servo motor and the electromagnetic suspension, are known.

C. Task III - Assembly of Apparatus and Development of Techniques

1. Prototype Apparatus

In order to gain experience with the performance of the various units of the apparatus, a prototype system has been constructed. Except for the small and large masses all the components of this prototype system are to be used in the final designs. The suspension is a 10 micron diameter tungsten fiber 30 cms in length.

An assembled view of the apparatus is shown in Figure 5. The precision spindle, S, is mounted in bearings attached to the granite surface plate, P. The rotary table, R, is mounted on a flange attached to the precision spindle. The stator for the servo control motor, m, is mounted to the bottom of the surface plate, while all other components are mounted on the top of the rotary table. The small mass system (not visible) is located within the vacuum jacket, V. The fiber is held on a clamp, C, with the plane of the dumbbell being roughly coincident with the imaginary center line of the large masses, L. A mirror is attached to the rigid dumbbell assembly, at the location of the windows W-W¹ which occurs just below the point of attachment of the suspension fiber to the dumbbell. The light source and optical lever systems are also mounted on the rotary table; D¹ being a coarse reading device and, D, a fine reading detector. It is planned to hold a static vacuum in the system during operation. The vacuum chamber will be pumped prior to the experiment through the port x, which will then be closed off and disconnected from the pumping system. G is a vacuum gauge.

This prototype apparatus is now being used to study the stability and noise level of the fiber suspension and as soon as the control loop for the servo motor is completed, some preliminary operations will begin.

2. Metrology

The problem of developing the measurement techniques required to determine to desired accuracy all of quantities involved in Eq. B page 6 so as to be able to insert this in Eq.A, page 5 and calculate G to high precision, is a major task. Considerable thought and study, both on our part and in consultation with others experienced and expert in the field, have gone into the design of the measurement techniques. No definite conclusions have as yet been reached. The delay here is not serious since the first 6-9 months of operation of the apparatus will be devoted to a study of various perturbation effects and will not

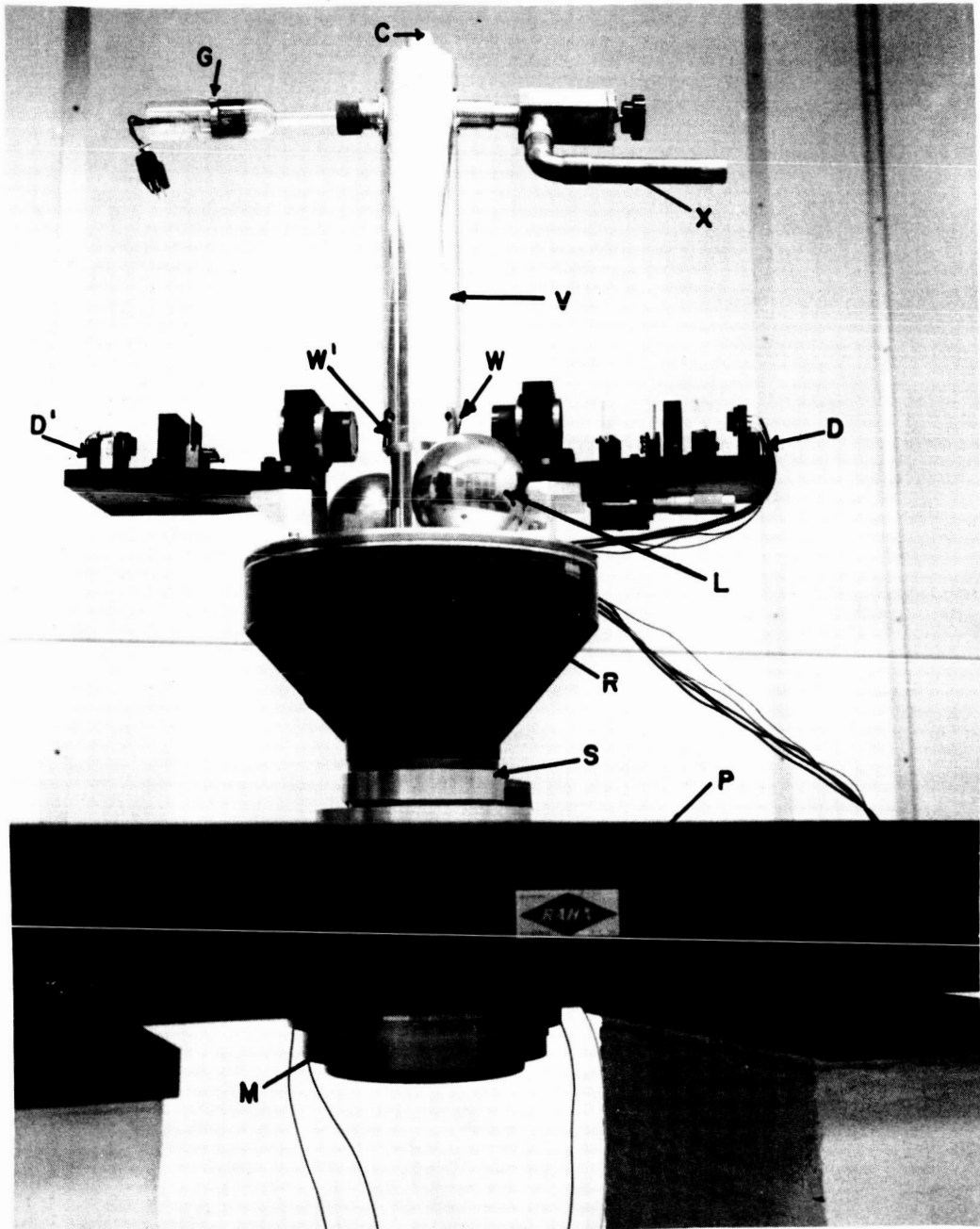


FIGURE 5
PROTOTYPE ASSEMBLY

require precision objects for the mass systems. The first technique required will be that for alignment of the mass system centers with the axis of rotation of the rotary table. Interferrometric methods are under study.

SECTION III STAFF

In addition to the principal investigators, the assistance of the following colleagues is gratefully acknowledged.

Drs. John Boring and Robert Humphris, members of the senior research staff of the Department of Aerospace Engineering and Engineering Physics, who have assumed responsibilities for various phases of the development.

Mr. James Dickerson, Design Engineer, who has developed the detailed specifications for many of the components procured commercially, and is supervising the design and construction of the first prototype and assisting with its checkout.

Mr. William Towler, Electronic Engineer, who is developing the servo control system for the rotary table, and the magnetic suspension system.

Miss Jo Anne Soderquist, a graduate student in Aerospace Engineering, who is performing the detailed calculations on many of the problems.

Finally, much gratitude is due to Dr. A. V. McNish and his staff at the National Bureau of Standards and Messers. Roger Hibbs and Ed Bailey at the Y-12 Plant, Union Carbide Corporation, Nuclear Division, Oak Ridge, Tennessee, for their time and interest in the project which has resulted in many helpful suggestions and deeds.

SECTION IV
EXPENDITURES

		<u>April 1 - Sept. 30</u>	<u>Total</u>
1.	Salaries and Labor	\$ 15,399.20	\$22,148.17
2.	Employee Benefits	1,257.01	1,977.96
3.	Machine Shop Services	3,881.38	3,930.18
4.	Reports Group Service	108.35	173.45
5.	Travel	34.71	84.72
6.	Materials and Supplies	1,995.02	2,774.40
7.	Communications	77.88	97.38
8.	Equipment	16,464.60	16,795.95
9.	Encumbrances*	<u>7,783.00</u>	<u>7,783.00</u>
	Subtotal	\$47,001.15	\$55,785.21
10.	Indirect Costs	<u>9,400.23</u>	<u>11,157.04</u>
	Total Expenditures	\$56,401.38	\$66,942.25

* The encumbrances are for the fabrication of the large mass system.

REFERENCES

1. See e. g.
Beams, J. W., "Ultra High Speed Rotation," Sci. American, 204, 134
April 1961.
Beams, J. W., "High Speed Rotation," Physics Today, 12, 20, July
1959.
2. Beams, J. W., Kuhlthau, A. R., Lowry, R. A. and Parker, H. M.,
"Determination of Newton's Gravitational Constant, G, with
Improved Precision," University of Virginia, Research Laboratories
for the Engineering Sciences, Proposal No. EP-NASA-125-64U,
submitted to NASA, June 1964.
3. Beams, J. W., Kuhlthau, A. R., Lowry, R. A., and Parker, H. M.,
Determination of Newton's Gravitational Constant, G, with
Improved Precision," Status Report No. 1, June 1965; University
of Virginia, Research Laboratories for the Engineering Sciences,
Report EP-4028-101-65U, NASA-CR-63796.
4. Boring, J. W., "Molecular-Surface Interactions at Satellite Velocities,"
University of Virginia, Research Laboratories for the Engineering
Sciences, Proposal No. AST-NASA-170-65U, submitted to NASA,
May 1965.
5. Pearson, S. and Wadsworth, N. J., "A Robust Torsion Balance which
Can Detect a Force of 2×10^{-8} Dyne," Jour. Sci. Inst. 42, 150,
1965.

DISTRIBUTION LIST

Copy No.

1 - 6	National Aeronautics and Space Administration Technical Reports Office Office of Grants and Research Contracts Washington, D. C. 20546
7 - 8	J. W. Beams
9	A. R. Kuhlthau
10	R. A. Lowry
11	H. M. Parker
12	J. W. Boring
13	R. R. Humphris
14	L. R. Quarles
15 - 20	RLES Files
21 - 22	University Library, Attn: J. C. Wyllie